A Novel Anti-inflammatory D-peptide Halts Disease Phenotype Progression in an Als Mouse Model

Julia Post
Forschungszentrum Jülich GmbH
Vanessa Kogel
Forschungszentrum Jülich GmbH
Anja Schaffrath
Forschungszentrum Jülich GmbH
Philipp Lohmann
Forschungszentrum Jülich GmbH
Nadim Joni Shah
Forschungszentrum Jülich GmbH
Karl-Josef Langen
Forschungszentrum Jülich GmbH
Dieter Willbold
Forschungszentrum Jülich GmbH
Antje Willuweit
Forschungszentrum Jülich GmbH
Janine Kutzsche (j.kutzsche@fz-juelich.de)
Forschungszentrum Julich GmbH https://orcid.org/0000-0003-0271-7390

Research

Keywords: Amyotrophic lateral sclerosis, behaviour, plasma cytokines, D-enantiomeric peptide, neuroinflammation, SOD1*G93A

DOI: https://doi.org/10.21203/rs.3.rs-30893/v1

Abstract

Background: Amyotrophic lateral sclerosis (ALS) is a progressive neurodegenerative disease characterised by selective neuronal death in brain stem and spinal cord. The cause is unknown, but an increasing evidence has firmly certified that neuroinflammation plays a key role in ALS pathogenesis. Neuroinflammation is a pathological hallmark of several neurodegenerative disorders and has been implicated as driver of disease progression. Here, we describe two treatment studies demonstrating the therapeutic potential of a tandem version of the well-known all-d-peptide RD2 (RD2RD2) in a transgenic mouse model of Alzheimer's disease (APP/PS1) and in a transgenic mouse model of ALS (SOD1*G93A).

Methods:APP/PS1 and SOD1*G93A mice were treated intraperitoneally for four weeks mice with RD2RD2 vs placebo. APP/PS1 brain and plasma samples were histologically and biochemically analysed for inflammatory markers, gliosis and amyloid pathology. SOD1*G93A mice were tested longitudinally during treatment in various behavioural and motor coordination tests. Brain and spinal cord samples were investigated immunohistochemically for gliosis and neurodegeneration.

Results: Treatment in APP/PS1 mice revealed significant reduction in glial cell activation in the brain and significantly lower levels of inflammatory cytokines in plasma. RD2RD2 treatment in SOD1*G93A mice resulted not only in a reduction of activated astrocytes and microglia in both brain stem and lumbar spinal cord but also in a rescue of neurons in the motor cortex. Moreover, behavioural tests revealed that the disease phenotype of SOD1*G93A mice is halted during treatment.

Conclusion: Based on the presented results, we conclude that RD2RD2 is a potential therapeutic candidate against ALS.

Background

Alzheimer's disease (AD), Parkinson's diseases (PD) and amyotrophic lateral sclerosis (ALS) are among the most common neurodegenerative diseases in adults. In addition to cognitive impairment, selective neuronal death and neuroinflammation in the central nervous system are prominent pathologic features in AD [1–4]. Clinically, ALS manifests as focal muscular weakness, with atrophy of skeletal muscles up to progressive paralysis and premature death, usually from respiratory failure [5]. Most ALS cases are sporadic (sALS), while a minority are familial cases (fALS) and caused by inherited mutations [6]. A key discovery was the identification of a mutation in the gene of the enzyme superoxide dismutase 1 (SOD1), which is causative in up to 20% of all fALS and in up to 3% of sALS cases [7, 8]. To investigate the pathophysiology of ALS and the role of mutated SOD1 in disease development and progression of ALS, a transgenic mouse model was created (tg(SOD1*G93A)1Gur), which expresses mutant SOD1 (SOD1*G93A) and develops adult-onset neurodegeneration of neurons in the lumbar spinal cord and motor cortex and progressive motor deficits, which leads to paralysis [9–12]. Due to similar clinical features and pathology to human ALS, these mice have been studied extensively over years and are still a cornerstone of preclinical ALS research [13]. In addition to the clinical symptoms, neuroinflammation and

immune-inflammatory processes are further prominent pathological hallmarks of human ALS cases and the transgenic SOD1*G93A mice [14–16]. Neuroinflammation is characterised by the presence of activated glial cells, mainly microglia and astrocytes. In addition, previous studies demonstrated that activated astrocytes and microglia play a role in disease progression of ALS [17, 18]. Cytokines, the primary messengers of inflammatory processes, are released by microglia and astrocytes in response to neuroinflammation [19–21]. They can be classified into two different types: Type 1 cytokines (= pro-inflammatory) increase the inflammatory reaction, while type 2 cytokines (= anti-inflammatory) decrease the inflammatory reaction. In a non-pathological state, a complex signalling cascade produces a protective immune response through cytokines [22, 23]. A temporal increased level of inflammatory cytokines was observed in ALS, but also in AD [24–26]. Like many other neurodegenerative diseases, such as AD, to date there is no curative therapy for ALS. Thus far, only symptomatic and minor life-prolonging treatments are available [27–29].

Recently, we have described the development of compounds for a disease-modifying treatment of AD. The compound RD2 binds preferentially amyloid beta (Aβ) monomers with nanomolar affinity and stabilizes Aβ in its native conformation [30], which is a novel strategy to directly disassemble toxic Aβ oligomers into native monomers [31]. RD2 has recently successfully passed a phase I clinical trial in healthy subjects (Single Ascending Doses (SAD) EUDRA-CT: 2017-000396-93 and Multiple Ascending Doses (MAD) EUDRA-CT: 2018-002500-14) [32] after demonstrating its preclinical efficacy in several AD mouse models [33–36]. The head-to-tail tandem version of RD2, RD2RD2, was designed to obtain a bivalent version of RD2 with potentially higher avidity and affinity for polyvalent Aβ assemblies. Like RD2, also RD2RD2 belongs to a relatively new class of drugs, the all-d-peptides, which consist solely of denantiomeric amino acid residues (Fig. 1) and which exhibit several advantages including high proteolytic stability and low immunogenicity [37, 38].

Here, we describe the results of a study with RD2RD2 in the transgenic AD mouse model APP/PS1, which resulted in a strong inhibition of neuroinflammation with regard to astrogliosis, microgliosis and cytokine levels. Therefore, the therapeutic potential of RD2RD2 was additionally examined in the ALS SOD1*G93A transgenic mouse model. For this purpose, we treated SOD1*G93A transgenic mice intraperitoneally for four weeks with RD2RD2 vs placebo and performed longitudinally various behavioural and motor coordination tests. Subsequently, brain stem and lumbar spinal cord of treated mice were immunohistochemically investigated.

Methods

Ethical approval

Comissioned by the Forschungszentrum Jülich a first study was performed with the contract research organisationPsychoGenics Inc. (Tarrytown, NY, USA) in accordance with PsychoGenics' Standard Operating Procedures. Procedures were approved by the Institutional Animal Care and Use Committee in accordance with the National Institute of Health Guide for the Care and Use of Laboratory Animals.

Integrity of the data was ensured through a quality control process.All animal experiments of the second study were performed in accordance with the German Law on the protection of animals (TierSchG §§ 7-9) and with permit from the local authority (Landesamt für Natur, Umwelt und Verbraucherschutz Nordrhein-Westfalen (LANUV), North Rhine-Westphalia, Germany; AZ 84-02.04.2015.A106 and AZ 84-02.04.2014.A423).

Animals

The double transgenic $APP_{swe+PS1/M146L}$ (APP/PS1) AD mouse model, introduced by *Holcomb et al.* in 1998 [39], were bred at PsychoGenics Inc. (Tarrytown, NY, USA). Mice were housed in mixed-genotype and treatment groups of four female mice in a controlled environment (12/12 h light/dark cycle, humidity maintained around 50% and a room temperature between 20 °C and 23 °C). Food and water was available *ad libitum*.

Transgenic SOD1*G93A mice and their non-transgenic (ntg) littermates were bred from male mice transgenic for human SOD1*G93A (B6.Cg-Tg(SOD1*G93A)1Gur/J mice, carrying a high copy number of the transgene, purchased from JAX (The Jackson Laboratory, ME, USA)) and female C57BL/6-J mice obtained from CRIVER (Charles River Laboratories, Sulzfeld, Germany).Progenies were analysed for presence of the human SOD1 gene by quantitative PCR, as previously described [40]. Copy numbers of the transgene were checked by calculation of the delta cycle threshold (CT) = $CT_{internal\ control}$ - $CT_{gene\ of\ interest}$. Female SOD1*G93A mice with a high copy number of the transgene were selected for stratified randomisation into equally groups. Housing of the animals was under the same terms at the animal facility of the Forschungszentrum Jülich as described previously [41, 35].

Drug candidate

The d-peptide RD2RD2 (sequence: ptlhthnrrrrrptlhthnrrrrr, 3.2 kDa) was purchased from peptides & elephants (Potsdam, Germany) and Cambridge Peptides (Cambridge Peptides, Birmingham, UK) as lyophilized powder with a minimal purity of 95%. The peptide consists of 24 d-enantiomeric amino acid residues with its C-terminus being amidated.

Treatments

In the first study, seven-months aged female APP/PS1 mice and their non-transgenic littermates were treated intraperitoneally by use of Alzet osmotic minipumps (Alzet osmotic minipumps, model #1004, Alzet, USA). Mice were treated with 14 mg/kg/d RD2RD2 (n = 15) or with physiological saline at pH 7.0 (placebo n = 15 and as control groupntg n = 13). RD2RD2 was dissolved in sterile physiological saline at pH 7.0 and placed in minipumps for 24 h prior to implantation. The next day, the pumps were implanted intraperitoneally. In short, mice were anesthetised with isoflurane, the skin and the muscle layer below

was cut in the midline and the pump was inserted in the abdominal cavity. Following placement of the pump, the wound was sutured. All mice received three days of carprofen treatment after surgery (day of surgery plus two days after). Mice were monitored regularly for possible complications related to the surgical intervention and were medically attended. The sutures were removed aseptically approximately 7 to10days after surgery.

In the second study, 12 weeks old female SOD1*G93A mice and their non-transgenic littermates were treated intraperitoneally using the same procedure as described above. SOD1*G93A mice were treated with 18.8 mg/kg/d RD2RD2 (n = 12) or with physiological saline at pH 7.0 (placebo n = 10 and ntg n = 13) as control groups.

Plasma collection

After four weeks of treatment, APP/PS1 and non-transgenic mice were deeply anaesthetised and monitored for loss of reflexes in which all the responses to external stimuli cease (verified by a toe pinch). The final collection of blood was done by terminal cardiac puncture. All blood samples were collected in K_2EDTA tubes and kept on ice for short-term storage. Within 15 min of blood collection, tubes were centrifuged for 10 min at 2.000 g in a refrigerated centrifuge. The supernatant (plasma) was extracted using a pipette and transferred into pre-labelled tubes. Samples were stored at - 80 °C.

Cytokine assay

Plasma samples from the transgenic APP/PS1 mice were measured using a Bio-Plex MAP kit (Bio-Rad Laboratories Inc., CA, USA). PsychoGenics Inc. (Tarrytown, NY, USA) carried out the measurement of the plasma samples of transgenic APP/PS1 mice (RD2RD2 n = 15 and placebo n = 15). The assay was performed according to manufacturer's protocol. The plasma samples were examined for seven specific inflammation markers: interleukin-1 beta (IL-1β), interleukin-6 (IL-6), interleukin-10 (IL-10), interleukin-12 heterodimer p70 (IL-12p70), interferon gamma (IFN-γ), tumor necrosis factor alpha (TNF-α) and the C-X-C motif ligand 1 (CXCL1). In general, values below the limit of detection (LoD) were excluded from analysis. Inflammatory marker data were presented as pictograms per millilitre (pg/mL).

Tissue collection

Following blood collections, brains of APP/PS1 and non-transgenic mice were harvested after perfusion with 20 mM phosphate-buffered saline (PBS), pH 7.4 at room temperature (RT) and post-immersion fixed in 4% paraformaldehyde in PBS, pH 7.4 at 4 °C for three days. Brains were cut saggitally in 40 µm sections using a vibratome (Leica Biosystems Nussloch GmbH, Wetzlar, Germany). Sections were stored in cryoprotective media (PBS with 30% ethylene glycol, 30% glycerol) until further processing.

At the end of the second study, SOD1*G93A and non-transgenic mice were sacrificed for histopathological analysis. Brains and spinal cords of all mice were removed and snap frozen in - 80 °C isopentane. Saggital brain sections of 20 µm were cut using a cryotome (Leica Biosystems Nussloch GmbH, Wetzlar, Germany). In addition, 12 µm transversal sections of the lumbar spinal cord were harvested. The left brain hemisphere and the lumbar spinal cord (L1-L5 tract) were used for immunohistological analysis. The lumbar region of the spinal cord was identified as described previously [42, 43].

Immunohistochemical analysis

AD pathology (antibody 6E10 for Aβ) and gliosis (antibodies Iba1 for microglia and GFAP for astrocytes) of eight months old APP/PS1 mice were assessed by immunohistochemical analysis. Immunolabelling was performed on free-floating sections. The sections were rinsed in PBS and incubated in 1% Triton X-100, 10% H_2O_2 in PBS for 20 min at RT. After another PBS rinse, sections were blocked in 10% normal horse serum in PBS for 1 hour at RT. Primary antibodies were solved in PBS (anti-6E10, 1:500, BioLegend, San Diego, USA; anti-Iba1, 1:500, Abcam, Cambridge, UK; anti-GFAP, 1:2000, DAKO Agilent Technologies, Santa Clara, USA) and brain sections were incubated overnight at 4 °C in a humid chamber.

Analogous to the immunohistochemical analysis of APP/PS1 mice, gliosis of astrocytes and microglia was assessed in the four months old SOD1*G93A mice. Furthermore, SOD1*G93A mice were investigated for neuronal nuclei (antibody NeuN) in the brain. Tissue sections were fixed with 4% paraformaldehyde and treated with 70% formic acid for antigen retrieval. The sections were rinsed and treated with 3% H_2O_2 in methanol for elimination of endogenous peroxidases. After a further washing step, sections were incubated with the primary antibody overnight at 4 °C in a humid chamber (GFAP: DAKO Agilent Technologies, Santa Clara, USA; NeuN: Merck Millipore, Darmstadt, Germany) or for two hours at RT (CD11b: Abcam, Cambridge, UK). Primary antibodies were solved 1:1000 in tris buffered saline with 1% Triton X-100 (TBST) with 1% bovine serum albumin (BSA) (GFAP and NeuN) or 1:2000 in tris buffered saline (TBS) with 1% BSA (CD11b).

Afterward, sections of APP/PS1 and SOD1*G93A mice were rinsed and incubated with biotinylated secondary anti-mouse or anti-rabbit antibody (1:1000 in PBST (APP/PS1) or TBST (SOD1*G93A) with 1% BSA (GFAP, Iba1 and NeuN) or in TBS with 1% BSA (CD11b), Sigma Aldrich, Germany)) for two hours at RT followed by 3, 3’-Diaminobenzidine (APP/PS1) enhanced with saturated nickel ammonium sulfate solution (SOD1*G93A). Immunohistochemical sections were mounted with DPX Mountant medium (Sigma Aldrich, Germany) after washing in an ascending alcohol series. Brain sections reacted with 6E10 were visualised with a secondary FITC tagged antibody and then coverslipped with ProLong Gold mounting medium (Thermo Fisher Scientific, MA, USA).

Quantification

Immunolabelled sections with GFAP and Iba1 of APP/PS1 mice were analysed with a digital Olympus BX50 microscope (Olympus America Inc., Center Valley, USA) and 6E10 sections with a BioRad laser scanning confocal microscope (Bio Rad Laboratories, CA, USA). Histopathology analyses in APP/PS1 were carried out in the hippocampus and cortex region of the brain (RD2RD2 n = 8, placebo n = 8 and ntg n = 4). A total of three sections (4 images per section) were analysed with ImageJ (NIH) to estimate the percentage area (%) of the neuropil occupied by 6E10 (Aβ plaques), Iba1 immunoreactive microglial cells per unit area (mm^2) and GFAP immunoreactivity (astrogliosis) as optical density (OD)[44-46]. Images of SOD1*G93A sections were taken with a LMD6000 microscope (Leica Camera, Germany) and LAS 4.0 software. Immunoreactive microglial cells (antibody CD11b) and astrogliosis (antibody GFAP) were determined as percentage area (%) of the neuropil occupied by GFAP or CD11b immunoreactivity or of neuron nuclei (antibody NeuN) as count per stained area using ImageJ (National Institute of Health, Bethesda, USA) and CellProfiler Analyst (Broad Institute, Boston, USA)[47]. To avoid deviations in the analysis of the region of interest, a standard circle or rectangle was created with the ImageJ program. Histopathology analyses in SOD1*G93A were carried out in brain stem and lumbar spinal cord. CD11b immunoreactive area was analysed in the brain stem and lumbar spinal cord (brain stem: 3 to 4 slides per mouse, placebo n = 10, RD2RD2 n = 12, ntg n = 13 and lumbar spinal cord: 4 to 8 slides per mouse, placebo n = 10, RD2RD2 n = 11, ntg n = 11). GFAP immunoreactive area was analysed in the brain stem and lumbar spinal cord (brain stem: 4 to 6 slides per mouse, placebo n = 9, RD2RD2 n = 11, ntg n = 13 and lumbar spinal cord: 4 to 8 slides per mouse, placebo n = 8, RD2RD2 n = 10, ntg n = 12). NeuN counts were analysed in the brain stem and motor cortex layers 2/3 and 5 (brain stem: 3 to 5 slides per mouse, placebo n = 8, RD2RD2 n = 11, ntg n = 11 and motor cortex: 4 to 5 slides per mouse, placebo n = 10, RD2RD2 n = 10, ntg n = 10).

Body weight of SOD1*G93A

The weight of the SOD1*G93A animals was recorded at least three times per week beginning prior to pump implantation. Weighing was always performed between 8 a.m. and 9 a.m. to avoid diurnal variations.

Behavioural assessments

SOD1*G93A mice were tested longitudinally in different behavioural set ups (SHIRPA and modified pole test). Each behavioural test of the SOD1*G93A mice was performed before treatment (baseline measurements) and one week after the implantation (first trial day: 8 d ± 1 d after implantation; criteria: general health, i.e. weight gain, look of fur, posture, and motor activity). Experimenter was blind to genotype or treatment. All tests were carried out at the same time of the day. Before each test, all mice were allowed to habituate in a single cage for 30 min. All mice were observed daily for disease progression.

Phenotype assessment

The primary screen of the SHIRPA test battery was used to assess the phenotype [48, 49]. This test consisted of the following subtests, which are scored by the experimenter and summed up to an individual SHIRPA score: restlessness, alertness, startle response, pinna reflex, corneal reflex, touch response, pain response, grooming, and apathy, abnormal body carriage, abnormal gait, loss of righting reflex, forelimb placing reflex, hanging behaviour, hind limb tremor. The last seven tests mentioned above represent motor abilities of the mice and are additionally summed up to a motor score. Mice were individually tested and scored in an arena of 42.5 cm x 18.0 cm x 26.5 cm (L x H x W). Scoring was defined from 0 (similar to ntg littermates) to 3 (extremely abnormal from ntg littermates).

Modified pole test

The modified pole test [41] is a sensitive functional test to measure early changes in the motor behaviour of the SOD1*G93A mice. The following modifications were realised: The mice were placed with the head downwards instead of upwards on a vertical pole (height 50 cm, diameter 1.2 cm, rough-surfaced) and their movement downwards was rated. The runs were scored from 0 to 3 (0 continuous run, 1 part-way runs, 2 slipping downwards and 3 falling down). This procedure was performed three times and the sum of all three scores was used for analysis.

Statistics

Statistical analysis were performed using GraphPad Prism 8 (GraphPad Software Inc., USA) and SigmaPlot Version 11 (Systat Software, Germany). Presentation of data as mean ± SEM (behavioural tests and histochemical analysis), $p > 0.05$ was considered as not significant (ns). Normal distribution of data was tested by use of Shapiro-Wilk normality test (SigmaPlot Version 11, Systat Software, Germany). Two-way repeated measurement (RM) ANOVA with Fisher's Least Significant Difference (LSD) post hoc analysis was used to analyse the results of the behavioural tests of SOD1*G93A mice (body weight, SHIRPA test,modified pole test). One-way measurement ANOVA was used to analyse the results of the histochemical analysis (quantification of both studies) and biochemical analysis (cytokine assay of APP/PS1 samples).

Results

Reduction of activated glia cells in the brain of treated APP/PS1 mice

In the first study female APP/PS1 mice were treated intraperitoneally for 4 weeks with either RD2RD2 or placebo. At the end of the treatment period brains were taken for immunohistological analyses of plaque

load and neuroinflammation. The RD2RD2-treated APP/PS1 mice displayed a mild tendency towards reduced Aβ deposits (antibody 6E10), but the difference was not statistically significant when compared to placebo-treated mice. No Aβ deposits were observed in the non-transgenic group (Fig. 2 g).

The APP/PS1 placebo group showed increased microglial cells (antibody Iba1) in the cortex and hippocampus in comparison to the non-transgenic and RD2RD2-treated mice. Treatment with RD2RD2 had a strong effect on neuroinflammation as itsignificantly reduced the number of activated microglia in both cortex and hippocampus down to levels of non-transgenic mice (Tab. 1 and Fig. 2 c and d). In addition, RD2RD2-treated mice displayed significantly reduced astrogliosis (antibody GFAP) in the cortex and hippocampus (Tab. 1 and Fig. 2e and f).

Table 1

Treatment with RD2RD2 significantly reduced gliosis in APP/PS1 mice. Analysis of amyloid deposits and activated glia cells in AD mice indicate a significant change in the neuroinflammatory pathology after intraperitoneal treatment with RD2RD2 compared to placebo-treated mice. Data is presented as mean ± SEM. Statistical calculations were conducted by one-way ANOVA with Fisher's LSD post hoc analysis. Lozenges (#) and Asterisks (*) indicate a significance between treatment groups (ntg vs RD2RD2 or ntg vs placebo: ### $p < 0.001$ and RD2RD2 vs placebo: * $p = 0.05$, ** $p = 0.01$, *** $p < 0.001$). IR: immunoreactivity, n/a: not analysed, OD: optical density

IR	Area	ntg	RD2RD2	placebo	Statistic (one-way ANOVA Analysis of Variance)
6E10 (%)	cortex	n/a	0.95 ± 0.08	1.05 ± 0.13	$F(1,14) = 0.48$, $p = 0.498$ RD2RD2 vs placebo $p = 0.498$ (ns)
	hippocampus	n/a	0.95 ± 0.10	1.02 ± 0.13	$F(1,14) = 0.23$, $p = 0.638$ RD2RD2 vs placebo $p = 0.638$ (ns)
Iba1 (counts)	cortex	228 ± 13.4	203 ± 13.2 ***	320 ± 14.1 ###	$F(2,17) = 25.57$, $p < 0.001$ ntg vs RD2RD2 $p = 0.876$ (ns) ntg vs placebo $p < 0.001$ RD2RD2 vs placebo $p < 0.001$
	hippocampus	200 ± 9.92	220 ± 16.2 ***	383 ± 12.1 ###	$F(2,17) = 42.28$, $p < 0.001$ ntg vs RD2RD2 $p = 0.722$ (ns) ntg vs placebo $p < 0.001$ RD2RD2 vs placebo $p < 0.001$

IR	Area	ntg	RD2RD2	placebo	Statistic (one-way ANOVA Analysis of Variance)
GFAP (OD)	cortex	117 ± 5.66	176 ± 9.66 ###, *	208 ± 9.92 ###	F(2,17) = 17.04, p < 0.001 ntg vs RD2RD2 p = 0.002 ntg vs placebo p < 0.001 RD2RD2 vs placebo p = 0.021
	hippocampus	228 ± 6.29	275 ± 12.4 **	357 ± 20.5 ###	F(2,17) = 13.70, p < 0.001 ntg vs RD2RD2 p = 0.097 (ns) ntg vs placebo p < 0.001 RD2RD2 vs placebo p = 0.001

Treatment of RD2RD2 inhibited up-regulation of cytokines in APP/PS1 mice

Cytokine levels in the blood of RD2RD2- and placebo-treated APP/PS1 mice were determined at the end of the study using the Bio-Plex MAP kit assay. Analysis of the inflammatory marker levels revealed a remarkable and significant decrease in the levels of all cytokines measured in RD2RD2-treated APP/PS1 mice in comparison to the placebo group (Tab. 2).

Table 2

Treatment with RD2RD2 significantly reduced levels of inflammatory markers in the blood of APP/PS1 mice. A Bio-Plex Map kit was used to analyse a possible change of inflammatory cytokines at the end of the study. Cytokine concentrations are given in picogram per milliliter (pg/mL). Data is presented as mean ± SEM. Statistical calculations were conducted by one-way ANOVA with Fisher's LSD post hoc analysis, RD2RD2 n = 15 and placebo n = 15 for each cytokine. Asterisks (*) indicate a significance between treatment groups (RD2RD2 vs placebo: *** $p < 0.001$)

Marker (pg/mL)	RD2RD2	placebo	Statistic (one-way ANOVA Analysis of Variance)
IL-1β	394 ± 57.6 ***	950 ± 60.4	$F(1,28) = 44.52$, $p < 0.001$ RD2RD2 vs placebo $p < 0.001$
IL-6	53.6 ± 7.87 ***	122 ± 6.75	$F(1,28) = 43.46$, $p < 0.001$ RD2RD2 vs placebo $p < 0.001$
IL-10	139 ± 18.9 ***	300 ± 16	$F(1,28) = 42.74$, $p < 0.001$ RD2RD2 vs placebo $p < 0.001$
IL-12p70	677 ± 88.5 ***	1612 ± 87.3	$F(1,28) = 56.55$, $p < 0.001$ RD2RD2 vs placebo $p < 0.001$
INF-γ	61 ± 8.87 ***	189 ± 7.34	$F(1,28) = 123.56$, $p < 0.001$ RD2RD2 vs placebo $p < 0.001$
CXCL-1	103 ± 9.79 ***	144 ± 6.25	$F(1,28) = 12.79$, $p = 0.001$ RD2RD2 vs placebo $p = 0.001$
TNF-α	517 ± 57.3 ***	1689 ± 107	$F(1,28) = 93.32$, $p < 0.001$ RD2RD2 vs placebo $p < 0.001$

Encouraged by the strong effect of RD2RD2 on neuroinflammation in treated APP/PS1 mice, we performed a second treatment study using the transgenic ALS mouse model SOD1*G93A, a model in which neuroinflammation has been described to drive disease progression [18, 19].

-

RD2RD2 treatment stopped motor phenotype progression without negative side effects in SOD1*G93A mice

Twelve weeks old female SOD1*G93A mice were treated with placebo (n = 10) or 18.8 mg/kg/d RD2RD2 (n = 12) formulated in an intraperitoneal osmotic minipump for 28 days. After a small weight loss post-operatively, all mice gained weight continuously over the four weeks treatment period. Throughout the whole testing period the average body weight was significantly different between non-transgenic and transgenic mice (Fig. 3 a; RD2RD2: 18.8 ± 0.2 g, placebo: 19.0 ± 0.2 g vs ntg: 20.3 ± 0.3 g; two-way RM ANOVA, $F(2,128) = 7.87$, $p = 0.002$, Fisher's LSD post hoc analysis, ntg vs RD2RD2 $p < 0.001$ and ntg vs placebo $p = 0.006$). RD2RD2 treatment neither influenced the average body weight nor body weight gain.

The SHIRPA test battery was used to monitor the progression of the neurodegenerative phenotype of transgenic placebo- or RD2RD2-treated mice. At baseline and during treatment, both transgenic groups showed behavioural and motor impairments compared to their non-transgenic littermates (Fig. 3 b; two-way RM ANOVA, $F(2,128) = 101.06$, $p < 0.001$, Fisher's LSD post hoc analysis, ntg vs RD2RD2 $p < 0.001$ and ntg vs placebo $p < 0.001$). Already after two weeks of treatment, the difference in SHIRPA score was statistically significant between the RD2RD2 group and placebo-treated SOD1*G93A mice (Fig 3 b; RD2RD2 vs placebo $p < 0.001$).

The subdivision of the SHIRPA parameters into a motor score revealed further specific details about progression of motor deficits of placebo- but not RD2RD2-treated mice (Fig. 3 c). At the end of the treatment period, motor deficits were significantlyloweruponRD2RD2 treatment in comparison to placebo-treated SOD1*G93A mice(Fig. 3 c; motor score, two-way RM ANOVA, $F(2,128) = 66.77$, $p < 0.001$, Fisher's LSD post hoc analysis, placebo vs ntg $p < 0.001$ and placebo vs RD2RD2 $p < 0.001$).

Additional investigations on the motor performance of RD2RD2-treated SOD1*G93A mice were performed with the pole test(Fig. 3 d). This test indicates functional deficits in motor coordination and muscular strength of SOD1*G93A mice. Throughout the experiment, non-transgenic mice did not show any motor deficits, while transgenic SOD1*G93A mice displayed already a significantly higher pole score at baseline (Fig. 3 d; two-way RM ANOVA, $F(2,128) = 104.95$, $p < 0.001$, Fisher's LSD post hoc analysis, ntg vs RD2RD2 $p < 0.001$ and ntg vs placebo $p < 0.001$). There was a slight but significant progression in the motor deficit of the placebo groupwhile the RD2RD2-treated SOD1*G93A mice kept their motor skills on a constant level (Fig. 3 d; two-way RM ANOVA, $F(1,80) = 0.85$, $p = 0.05$, Fisher's LSD post hoc analysis, RD2RD2 vs placebo (treatment week 4) $p = 0.021$).

RD2RD2 treatment led to reduction of activated glia cells and restored neuron density in SOD1*G93A mice

To support the findings of the SHIRPA and pole test of RD2RD2-treated SOD1*G93A mice, we analysed activation of inflammatory cells in the brain stem, as well as neuronal nuclei in the motor cortex of all mice. Moreover, we analysed sections of the lumbar spinal cord, since motor weakness is first detectable in the hind limbs in this mouse model and the motoric pathways are linked through the lumbar spinal cord to the brain. For pathological analysis, levels of activated glia cells (using antibodies CD11b for activated microglia and GFAP for activated astrocytes) and the number of neurons (using antibody NeuN) were determined by immunohistochemical staining and quantified. Immunolabelling revealed a significantly decreased number of activated microglia in the brain stem of RD2RD2-vs placebo-treated SOD1*G93Amice (Tab. 3and Fig. 4 a). In lumbar spinal cord sections from RD2RD2-treated SOD1*G93A mice activated microgliashowed also a decrease which did not reach statistical significance towards placebo-treated animals (Tab. 3 and Fig. 4 b). Additionally, we analysed activated astrocytes. There was a significant difference in the number of activated astrocytes in the brain stem between all three treatment groups after 28 days of treatment (Tab. 3 and Fig. 4 c). RD2RD2 treatment was able to reduce also the number of activated astrocytes significantly in comparison to the placebo group. More important, analysis of activated astrocytes within the lumbar spinal cord revealed a significant decrease in the RD2RD2-treated SOD1*G93A mice down to levels which are not significant to non-transgenic littermates (Tab. 3 and Fig. 4 d).

Table 3

Evaluation of immunolabelling in brain and lumbar spinal cord of SOD1*G93A mice revealed a decrease of gliosis after treatment with RD2RD2. Data is presented as mean ± SEM. Statistical calculations were conducted by one-way ANOVA with Fisher's LSD post hoc analysis. Lozenges ($^{\#}$) and asterisks (*) indicate a significance between treatment groups (ntg vs RD2RD2 or ntg vs placebo: $^{\#}$ p = 0.05, $^{\#\#}$ p = 0.01, $^{\#\#\#}$ p < 0.001 and RD2RD2 vs placebo: * p = 0.05, *** p < 0.001). IR: immunoreactivity

IR	Area	ntg	RD2RD2	placebo	Statistic (one-way ANOVA Analysis of Variance)
CD11b (%)	brain stem	1.21 ± 0.13	2.41 ± 0.28 $^{\#,***}$	4.29 ± 0.54 $^{\#\#\#}$	F(2,32) = 22.02, p < 0.001 ntg vs RD2RD2 p = 0.011 ntg vs placebo p < 0.001 RD2RD2 vs placebo p < 0.001
	lumbar spinal cord	0.46 ± 0.07	1.00 ± 0.23	1.57 ± 0.44 $^{\#\#}$	F(2,29) = 3.96, p = 0.030 ntg vs RD2RD2 p = 0.175 (ns) ntg vs placebo p = 0.009 RD2RD2 vs placebo p = 0.156 (ns)
GFAP (%)	brain stem	1.43 ± 0.16	3.23 ± 0.37 $^{\#\#,*}$	4.68 ± 0.88 $^{\#\#\#}$	F(2,30) = 11.62, p < 0.001 ntg vs RD2RD2 p = 0.009 ntg vs placebo p < 0.001 RD2RD2 vs placebo p = 0.049

IR	Area	ntg	RD2RD2	placebo	Statistic (one-way ANOVA Analysis of Variance)
	lumbar spinal cord	0.73 ± 0.08	1.69 ± 0.4 *	3.16 ± 0.6 ###	F(2,27) = 10.93, p < 0.001 ntg vs RD2RD2 p = 0.060 (ns) ntg vs placebo p < 0.001 RD2RD2 vs placebo p = 0.011
NeuN (counts)	brain stem	450 ± 42.3	406 ± 31.8 ##,*	343 ± 46.4 ###	F(2,27) = 1.66, p = 0.208 ntg vs RD2RD2 p = 0.002 ntg vs placebo p < 0.001 RD2RD2 vs placebo p = 0.021
	motor cortex	947 ± 42.8	924 ± 32.9 *	784 ± 42.6 ##	F(2,27) = 4.92, p = 0.015 ntg vs RD2RD2 p = 0.677 (ns) ntg vs placebo p = 0.007 RD2RD2 vs placebo p = 0.020

Moreover, we analysed the number of neurons in SOD1*G93A mice in brain stem and motor cortex(Tab. 3). Quantification of NeuN-positive cells revealed a loss of neurons in transgenic SOD1*G93A mice vs non-transgenic littermates in both regions. Treatment with RD2RD2 significantly rescued neurons in motor cortex to levels of non-transgenic littermates. The number of neurons in brain stem showed the same, but non-significant, tendency (Tab. 3).

Discussion

AD and ALS are both fatal neurodegenerative diseases affecting the central nervous system. Despite intensive research, current treatment options are only symptomatic [50, 29]. Neuroinflammation plays a major role in both diseases, increasing evidence has firmly certified that neuroinflammation induced by Aβ plays a key role in the pathogenic process in AD [51, 52], as well as induced by SOD1 in ALS pathogenesis [14, 25].

In the hereby described work, we examined the compound RD2RD2 for its therapeutic efficacy in neurodegenerative diseases, like AD or ALS. RD2RD2 has been discovered in a screening campaignagainst Aβ and was able to reduce Aβ induced cell toxicity *in vitro*[33]. Based on these promising characteristics an *in vivo* study with RD2RD2 in an AD specific mouse model was initiated.Intraperitoneal treatment of seven-months aged APP/PS1 mice for 28 days with RD2RD2 had no significant impact on plaque load in cortex and hippocampus, but a remarkable effect on neuroinflammation. In the cortex and hippocampus of treated APP/PS1 mice, the numbers of activated microglia cells were reduced close to the level of non-transgenic littermates. Also, astrogliosis was significantly reduced in both areas.A high number of GFAP-positive astrocytes and Iba1-positive microglia near the developing Aβ deposits in the cortex has been described in this mouse model at the age of six months [53]. At the end of the treatment, the APP/PS1 mice were eight months old and plaque pathology was developed as expected. However, no significant effect of the treatment on the amount of amyloid plaques was found. Instead, the plasma levels of all tested inflammatory cytokines were reduced upon RD2RD2 treatment. Activation of glial cells has been shown to influencethe release of pro- and anti-inflammatory cytokines [4]. The significant decrease of cytokine levels in RD2RD2-treated APP/PS1 mice were associated with their significant lower activation of glial cells in the brain and suggest that although ineffective on Aβ pathology RD2RD2 acts as an anti-inflammatory compound.

Based on these promising anti-inflammatory effects in the APP/PS1 AD mouse model, we decided to continue the treatment in another mouse model of a neurodegenerative disorder in which neuroinflammation is known as main driver of the disease. Therefore, the SOD1*G93A ALS mouse model was chosen [17, 18, 26, 54]. SOD1*G93A mice were treated intraperitoneally for 28 days with RD2RD2 or placebo. RD2RD2 treatment of SOD1*G93A mice retarded significantly their phenotype progression, as measured using the SHIRPA test battery, in comparison to placebo-treated littermates. While the placebo-treated mice showed a significant progression of their phenotype within the four weeks treatment period, RD2RD2 treatment was able to completely stop progression of the disease phenotype and especially the motor deficits. Significant changes between the groups were already apparent after two treatment weeks. Further investigations on motor deficits were conducted by the modified pole test, a test measuring complex motor behaviour. Impairment of the motor skills of SOD1*G93A mice progressed slowly but significantly in the placebo group, but not in the RD2RD2-treated group.

In addition to the clinical symptoms like motor deficits, neuroinflammation is one prominent pathological hallmark of ALS and previous studies demonstrated the key role of activated astrocytes and microglia

cells in disease progression [17, 21]. In analogy of our observation in APP/PS1 mice, RD2RD2 treatment led to decreased levels of gliosis in brain stem and lumbar spinal cord in RD2RD2-treated SOD1*G93A mice vs placebo-treated littermates, indicating that RD2RD2 treatment reduced neuroinflammation also in this disease model. Furthermore, we investigated the density of neurons in the motor cortex and brain stem. Motor cortex neurons regulate the control of motor output and selectively degenerate in ALS [55]. During disease progression, degeneration of neurons of the motor cortex and brain stem causes muscle weakness and deficits in motor performance. Analysis of the neuronal nuclei in brain stem and motor cortex revealed a loss of neurons in SOD1*G93A mice in comparison to non-transgenic littermates, as described previously by others [56, 57]. However, there was a significantly higher density of neurons in both the motor cortex and brain stem of RD2RD2- vs placebo-treated mice. This supports our assumption that RD2RD2 has also an effect on neuronal survival in this mouse model of ALS.

The compound RD2 binds preferentially Aβ monomers with nanomolar affinity and stabilizes Aβ in its native conformation[30]. The rational for developing RD2RD2 was to obtain a bivalent version of RD2 with potentially higher avidity and affinity for polyvalent Aβ assemblies, like Aβ oligomers. However, RD2RD2 was not significantly efficient neither on amyloid load (Fig. 2) nor on cognitive deficits [34]. Instead,we found potent anti-inflammatory effects in the AD mouse model, which was confirmed in the ALS mouse model, although the mechanism of action is not yet clear. Since SOD1*G93A mice only secrete endogenous murine Aβ which is not capable of forming aggregates [58], an Aβ-mediated mechanism of action for RD2RD2 is unlikely. Therefore, an off-target effect of RD2RD2 on a so far unknown target can be assumed.

Conclusion

In summary, RD2RD2 demonstrated therapeutic efficacy in the SOD1*G93A ALS mouse model. Treatment with RD2RD2 led to a reduction of activated glia cell levels in the brain stem and lumbar spinal cord in SOD1*G93A mice. Analysis of neurons in the brain revealed a neuroprotective function of RD2RD2 in treated mice. The phenotype progression of SOD1*G93A mice was halted during the treatment. So far, the direct target of RD2RD2 is unknown. Therefore, future studies will focus on how RD2RD2 affects neuroinflammation and ALS pathogenesis. However, based on the presented results, we conclude that RD2RD2 is a potential therapeutic candidate against ALS.

Abbreviations

Aβ:	amyloid beta
AD:	Alzheimer's disease
ALS:	amyotrophic lateral sclerosis
APP/PS1:	$APP_{swe+PS1/M146L}$ transgenic mouse model
CD11b:	integrin alpha M subunit
CXCL1:	C-X-C motif ligand 1
fALS:	familial amyotrophic lateral sclerosis
GFAP:	glial fibrillary acidic protein
Iba1:	ionized calcium-binding adapter molecule 1
IL:	interleukin
INF:	interferon
IR:	immunoreactivity
i.p.:	intraperitoneal
NeuN:	neuronal nuclei
ntg:	non-transgenic
MAD:	Multiple Ascending Dose
OD:	optical density
SAD:	Single Ascending Dose
sALS:	sporadic amyotrophic lateral sclerosis
SOD1:	superoxide dismutase 1
TNF:	tumor necrosis factor
tg:	transgenic

Declarations

Acknowledgements

Not applicable.

Authors' Contribution

JK, AW and DW designed and planned the study. All in vivo experiments were performed by JP with support by VK. Immunohistochemical experiments were performed by JP and AS. Cytokine assay of AD samples was conducted by PsychoGenics Inc.. Evaluation and statistical analysis was done by JP and AW. The manuscript was written by JP, JK, AW and DW. All authors read and approved the final manuscript.

Funding

DW was supported by grants from the Russian Science Foundation (RSF) (project no. 20-64-46027) and by the Technology Transfer Fund of the Forschungszentrum Jülich. K-JL and DW were supported by "Portfolio Drug Research" of the "Impuls und Vernetzungs-Fonds der Helmholtzgemeinschaft".

Availability of data and materials

The datasets used and/or analysed during the current study are available from the corresponding author on reasonable request.

Corresponding authors'

Correspondence to j.kutzsche@fz-juelich.de

Ethics declarations

Ethics approval

All applicable international, national, and/or institutional guidelines for the care and use of animals were followed. All procedures performed in studies involving animals were in accordance with the ethical standards of the institution or practice at which the studies were conducted. All animal experiments at the contract research organisation PsychoGenics Inc. (Tarrytown, NY, USA) were performed in accordance with PsychoGenics' Standard Operating Procedures. Procedures were approved by the Institutional Animal Care and Use Committee in accordance with the National Institute of Health Guide for the Care and Use of Laboratory Animals. Integrity of the data was ensured through a quality control process. All animal experiments at the Forschungszentrum Jülich were performed in accordance with the German Law on the protection of animals (TierSchG §§ 7-9) and were approved by a local ethics committee (LANUV, North-Rhine-Westphalia, Germany, reference number: AZ 84-02.04.2015.A106 and AZ 84-02.04.2014.A423).

Consent for publication

Not applicable.

Competing interests

The authors declare that they have no competing interests. DW is co-inventor of patents covering the composition of matter of RD2RD2. DW and AW are co-founders and shareholders of the company “Priavoid GmbH”, which is planning to further develop RD2RD2.

References

1. Cacquevel M, Lebeurrier N, Chéenne S, Vivien D. Cytokines in neuroinflammation and Alzheimer's disease. Curr Drug Targets. 2004;5:529-34.
2. Maeda J, Ji B, Irie T, Tomiyama T, Maruyama M, Okauchi T, et al. Longitudinal, quantitative assessment of amyloid, neuroinflammation, and anti-amyloid treatment in a living mouse model of Alzheimer's disease enabled by Positron Emission Tomography. J Neurosci.2007;27:10957-68.
3. Paula A, Rodrigo AC, Catarina O. Neuroinflammation, Oxidative Stress and the Pathogenesis of Alzheimers Disease. Curr Pharm Des. 2010;16:2766-78.
4. Heneka MT, Carson MJ, Khoury JE, Landreth GE, Brosseron F, Feinstein DL, et al. Neuroinflammation in Alzheimer's disease. Lancet Neurol. 2015;14:388-405.
5. Mitchell JD, Borasio GD. Amyotrophic lateral sclerosis. The Lancet 2007;369:2031-41.
6. Cleveland DW, Rothstein JD. From charcot to lou gehrig: Deciphering selective motor neuron death in ALS. Nat Rev Neurosci.2001;2:806-19.
7. Deng HX, Hentati A, Tainer JA, Iqbal Z, Cayabyab A, Hung WY, et al. Amyotrophic lateral sclerosis and structural defects in Cu,Zn superoxide dismutase. Science. 1993;261:1047-51.
8. Rosen DR, Siddique T, Patterson D, Figlewicz DA, Sapp P, Hentati A, et al. Mutations in Cu/Zn superoxide dismutase gene are associated with familial amyotrophic lateral sclerosis. Nature. 1993;362:59-62.
9. Gurney ME, Pu H, Chiu AY, Dal Canto MC, Polchow CY, Alexander DD, et al. Motor neuron degeneration in mice that express a human Cu, Zn superoxide dismutase mutation. Science. 1994;264:1772-5.
10. Gurney ME. The use of transgenic mouse models of amyotrophic lateral sclerosis in preclinical drug studies. J Neurol Sci.1997;152:67-73.
11. Wang L, Sharma K, Deng H-X, Siddique T, Grisotti G, Liu E, et al. Restricted expression of mutant SOD1 in spinal motor neurons and interneurons induces motor neuron pathology. Neurobiol Dis. 2008;29:400-8.

12. Özdinler PH, Benn S, Yamamoto TH, Güzel M, Brown RH, Macklis JD. Corticospinal motor neurons and related subcerebral projection neurons undergo early and specific neurodegeneration in hSOD1G93A transgenic ALS mice. J Neurosci. 2011;31:4166-77.
13. Rothstein J. Current hypotheses for the underlying biology of amyotrophic lateral sclerosis. Ann Neurol. 2009;65 Suppl 1.
14. Philips T, Robberecht W. Neuroinflammation in amyotrophic lateral sclerosis: role of glial activation in motor neuron disease. Lancet Neurol.2011;10:253-63.
15. Robberecht W, Philips T. The changing scene of amyotrophic lateral sclerosis. Nat Rev Neurosci. 2013;14:248.
16. Jara JH, Genç B, Stanford MJ, Pytel P, Roos RP, Weintraub S, et al. Evidence for an early innate immune response in the motor cortex of ALS. J Neuroinflammation. 2017;14:129.
17. Boillée S, Yamanaka K, Lobsiger CS, Copeland NG, Jenkins NA, Kassiotis G, et al. Onset and progression in inherited ALS determined by motor neurons and microglia. Science. 2006;312:1389-92.
18. Hensley K, Abdel-Moaty H, Hunter J, Mhatre M, Mou S, Nguyen K, et al. Primary glia expressing the G93A-SOD1 mutation present a neuroinflammatory phenotype and provide a cellular system for studies of glial inflammation. J Neuroinflammation. 2006;3:2.
19. Patel NS, Paris D, Mathura V, Quadros AN, Crawford FC, Mullan MJ. Inflammatory cytokine levels correlate with amyloid load in transgenic mouse models of Alzheimer's disease. J Neuroinflammation. 2005;2:9.
20. Heneka MT, Kummer MP, Stutz A, Delekate A, Schwartz S, Vieira-Saecker A, et al. NLRP3 is activated in Alzheimer's disease and contributes to pathology in APP/PS1 mice. Nature. 2012;493:674.
21. Lewis C-A, Manning J, Rossi F, Krieger C. The Neuroinflammatory Response in ALS: The roles of microglia and T cells. Neurol Res Int. 2012;803701.
22. Greenhalgh CJ, Hilton DJ. Negative regulation of cytokine signaling. J LeukocBiol. 2001;70:348-56.
23. Turner MD, Nedjai B, Hurst T, Pennington DJ. Cytokines and chemokines: At the crossroads of cell signalling and inflammatory disease. Biochimica et Biophysica Acta (BBA) - Mol Cell Res. 2014;1843:2563-82.
24. Elliott JL. Cytokine upregulation in a murine model of familial amyotrophic lateral sclerosis. Mol Brain Res. 2001;95:172-8.
25. McGeer PL, McGeer EG. Inflammatory processes in amyotrophic lateral sclerosis. Muscle & Nerve. 2002;26:459-70.
26. Jeyachandran A, Mertens B, McKissick EA, Mitchell CS. Type I vs. Type II cytokine levels as a function of SOD1 G93A mouse amyotrophic lateral sclerosis disease progression. Front Cell Neurosci. 2015;9.
27. Brooks BR, Miller RG, Swash M, Munsat TL. El Escorial revisited: revised criteria for the diagnosis of amyotrophic lateral sclerosis. Amyotroph Lateral Scler and Other Motor Neuron Disord. 2000;1:293-9.

28. Miller RG, Mitchell J, Moore DH. Riluzole for amyotrophic lateral sclerosis (ALS)/motor neuron disease (MND). The Cochrane Library. 2012.
29. Dorst J, Ludolph AC, Huebers A. Disease-modifying and symptomatic treatment of amyotrophic lateral sclerosis. Ther Adv Neurol Disord. 2018;11:1-16.
30. Zhang T, Loschwitz J, Strodel B, Nagel-Steger L, Willbold D. Interference with amyloid-β nucleation by transient ligand interaction. Molecules. 2019;24:2129.
31. Willbold D, Kutzsche J. Do We Need Anti-Prion Compounds to Treat Alzheimer's Disease? Molecules. 2019;24:2237.
32. Kutzsche J, Jürgens D, Willuweit A, Adermann K, Fuchs C, Simons S, et al. Safety and pharmacokinetics of the orally available antiprionic compound PRI-002: A single and multiple ascending dose phase I study. Alzheimers Dement. 2020;6(1):e12001.
33. van Groen T, Schemmert S, Brener O, Gremer L, Ziehm T, Tusche M, et al. The Aβ oligomer eliminating d-enantiomeric peptide RD2 improves cognition without changing plaque pathology. Sci Rep. 2017;7:16275.
34. Kutzsche J, Schemmert S, Tusche M, Neddens J, Rabl R, Jürgens D, et al. Large-Scale Oral treatment study with the four most promising D3-derivatives for the treatment of Alzheimer's disease. Molecules. 2017;22:1693.
35. Schemmert S, Schartmann E, Zafiu C, Kass B, Hartwig S, Lehr S, et al. Aβ oligomer elimination restores cognition in transgenic Alzheimer's mice with full-blown pathology. MolNeurobiol. 2018; 56: 2211-2223.
36. Schemmert S, Schartmann E, Honold D, Zafiu C, Ziehm T, Langen KJ, et al. Deceleration of the neurodegenerative phenotype in pyroglutamate-Aβ accumulating transgenic mice by oral treatment with the Aβ oligomer eliminating compound RD2. Neurobiol Dis. 2019;124:36-45.
37. Leithold LHE, Jiang N, Post J, Niemietz N, Schartmann E, Ziehm T, et al. Pharmacokinetic properties of tandem d-peptides designed for treatment of Alzheimer's disease. Eur J Pharm Sci.2016;89:31-8.
38. Elfgen A, Hupert M, Bochinsky K, Tusche M, González de San Román Martin E, Gering I, et al. Metabolic resistance of the d-peptide RD2 developed for direct elimination of amyloid-β oligomers. Sci Rep. 2019;9:5715.
39. Holcomb L, Gordon MN, McGowan E, Yu X, Benkovic S, Jantzen P, et al. Accelerated Alzheimer-type phenotype in transgenic mice carrying both mutant amyloid precursor protein and presenilin 1 transgenes. Nat Med. 1998;4:97-100.
40. Ohgomori T, Yamasaki R, Takeuchi H, Kadomatsu K, Kira JI, Jinno S. Differential activation of neuronal and glial STAT3 in the spinal cord of the SOD1G93A mouse model of amyotrophic lateral sclerosis. Eur J Neurosci. 2017;46:2001-14.
41. Dunkelmann T, Schemmert S, Honold D, Teichmann K, Butzküven E, Demuth HU, et al. Comprehensive characterization of the pyroglutamate amyloid-β induced motor neurodegenerative phenotype of TBA2.1 mice. J Alzheimer's Dis. 2018;63:115-30.

42. Tadros MA, Harris BM, Anderson WB, Brichta AM, Graham BA, Callister RJ. Are all spinal segments equal: intrinsic membrane properties of superficial dorsal horn neurons in the developing and mature mouse spinal cord. J Physiol. 2012;590:2409-25.
43. Hugnot JP. Isolate and culture neural stem cells from the mouse adult spinal cord. NPC: Springer. 2013. p. 53-63.
44. Webster B, Hansen L, Adame A, Crews L, Torrance M, Thal L, et al. Astroglial activation of extracellular-regulated kinase in early stages of Alzheimer disease. J Neuropath Exp Neur. 2006;65:142-51.
45. Hwang I, Hoon Choi J, Li H, Yoo KY, Won Kim D, Hyun Lee C, et al. Changes in glial fibrillary acidic protein immunoreactivity in the dentate gyrus and hippocampus proper of adult and aged dogs. J Vet Med Sci. 2008;70:965-9.
46. Ferreira T, Rasband W. The ImageJ User Guide. 2011.
47. McQuin C, Goodman A, Chernyshev V, Kamentsky L, Cimini BA, Karhohs KW, et al. CellProfiler 3.0: Next-generation image processing for biology. PLOS Biol. 2018;16:e2005970.
48. Rogers DC, Fisher EMC, Brown SDM, Peters J, Hunter AJ, Martin JE. Behavioral and functional analysis of mouse phenotype: SHIRPA, a proposed protocol for comprehensive phenotype assessment. Mamm Genome.1997;8:711-3.
49. Rogers DC, Peters J, Martin JE, Ball S, Nicholson SJ, Witherden AS, et al. SHIRPA, a protocol for behavioral assessment: validation for longitudinal study of neurological dysfunction in mice. Neurosci. Lett. 2001;306:89-92.
50. Cummings J, Lee G, Ritter A, Zhong K. Alzheimer's disease drug development pipeline: 2018. Alzheimer's & Dementia: TRCI. 2018;4:195-214.
51. Miao J, Xu F, Davis J, Otte-Höller I, Verbeek MM, Van Nostrand WE. Cerebral microvascular amyloid-β protein deposition induces vascular degeneration and neuroinflammation in transgenic mice expressing human vasculotropic mutant amyloid-β precursor protein. Am. J. Pathol. 2005;167:505-15.
52. Craft JM, Watterson DM, Van Eldik LJ. Human amyloid β-induced neuroinflammation is an early event in neurodegeneration. Glia. 2006;53:484-90.
53. Gordon MN, Holcomb LA, Jantzen PT, DiCarlo G, Wilcock D, Boyett KW, et al. Time course of the development of Alzheimer-like pathology in the doubly transgenic PS1+APP mouse. Exp Neurol. 2002;173:183-95.
54. Lewis KE, Rasmussen AL, Bennett W, King A, West AK, Chung RS, et al. Microglia and motor neurons during disease progression in the SOD1G93A mouse model of amyotrophic lateral sclerosis: changes in arginase1 and inducible nitric oxide synthase. J Neuroinflammation. 2014;11:55.
55. Fogarty MJ, Noakes PG, Bellingham MC. Motor cortex layer V pyramidal neurons exhibit dendritic regression, spine loss, and increased synaptic excitation in the presymptomatic hSOD1G93Amouse model of amyotrophic lateral sclerosis. J Neuroscience. 2015;35:643-7.

56. An T, Shi P, Duan W, Zhang S, Yuan P, Li Z, et al. Oxidative stress and autophagic alteration in brainstem of SOD1-G93A mouse model of ALS. Mol Neurobiology. 2014;49:1435-48.
57. Solomonov Y, Hadad N, Levy R. Reduction of cytosolic phospholipase A2α upregulation delays the onset of symptoms in SOD1G93A mouse model of amyotrophic lateral sclerosis. J Neuroinflammation. 2016;13:134.
58. Jankowsky JL, Younkin LH, Gonzales V, Fadale DJ, Slunt HH, Lester HA, et al. Rodent Aβ modulates the solubility and distribution of amyloid deposits in transgenic mice. J Biol Chem. 2007;282:22707-20.

Figures

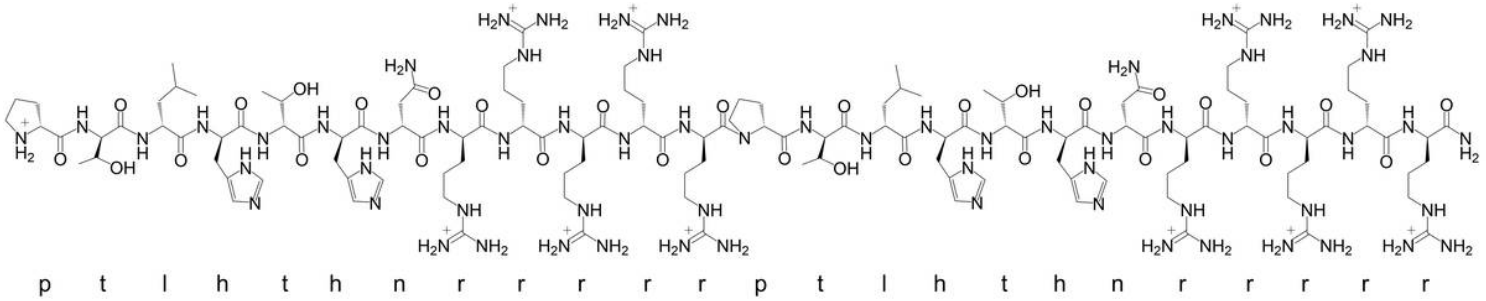

Figure 1

Lewis structure and single letter amino acid code of the D-enantiomeric peptide RD2RD2 (3.2 kDa).

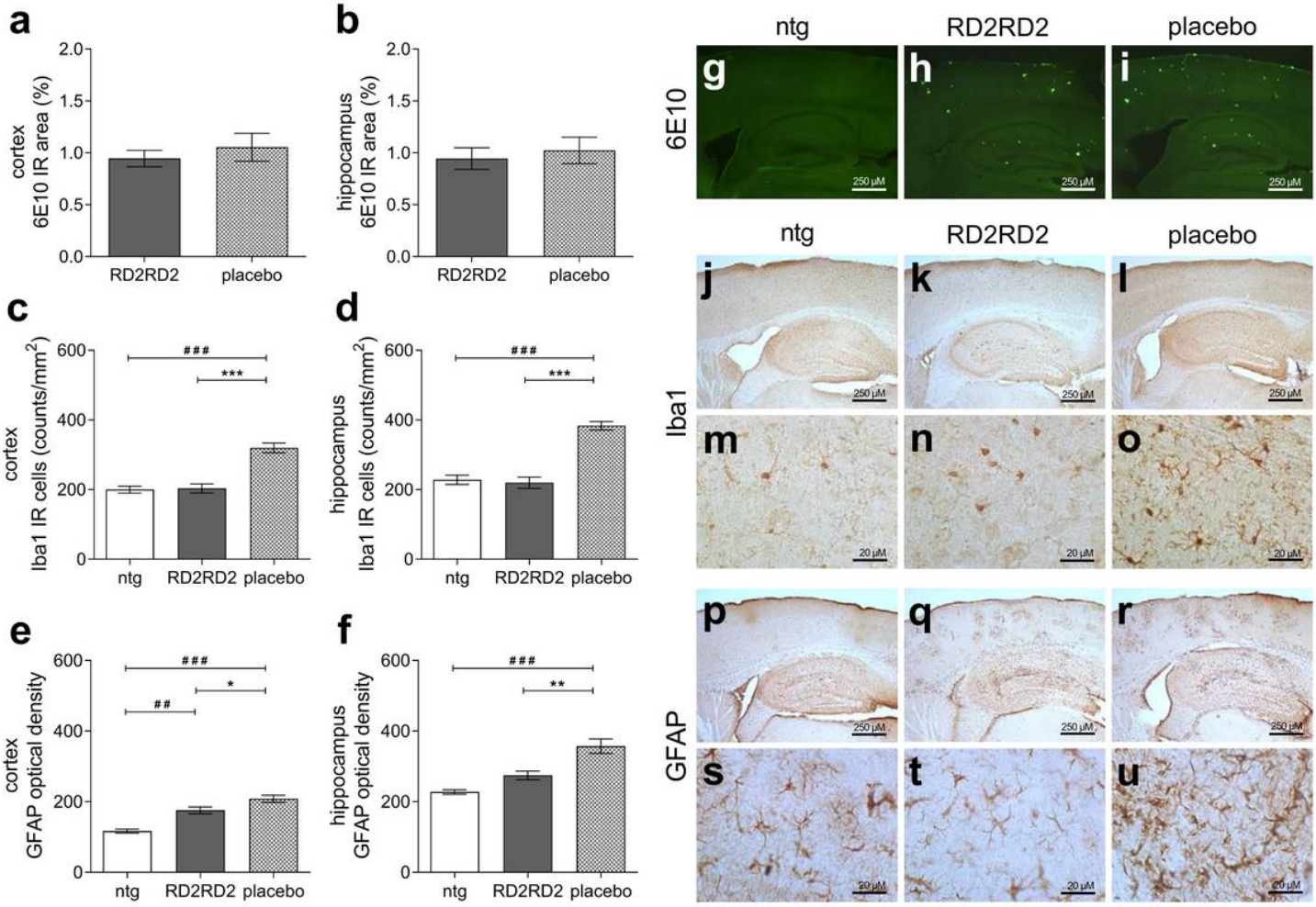

Figure 2

Analysis of amyloid pathology and neuroinflammation in cortex and hippocampus of RD2RD2-treated APP/PS1 mice.Treatment with RD2RD2 significantly reduced both the number of activated microglia (antibody Iba1) and of activated astrocytes (antibody GFAP) in the cortex and hippocampus of APP/PS1 mice. Plaque load (antibody 6E10) was not changed significantly upon RD2RD2 treatment. Presentation of the analysed cells and brain regions are given on the right (Aβ deposits: a, g-i = cortex and b = hippocampus; microglia: c, j-l = cortex and d, m-o = hippocampus; astrocytes: e, p-r = cortex and f, s-u = hippocampus). Data is presented as mean ± SEM. Statistical calculations were conducted by one-way ANOVA with Fisher's LSD post hoc analysis. Lozenges (#) and asterisks (*) indicate a significance between treatment groups (ntg vs RD2RD2 or ntg vs placebo:## $p < 0.01$, ### $p < 0.001$ and RD2RD2 vs placebo: * $p = 0.05$, ** $p = 0.01$, *** $p< 0.001$). IR: immunoreactivity

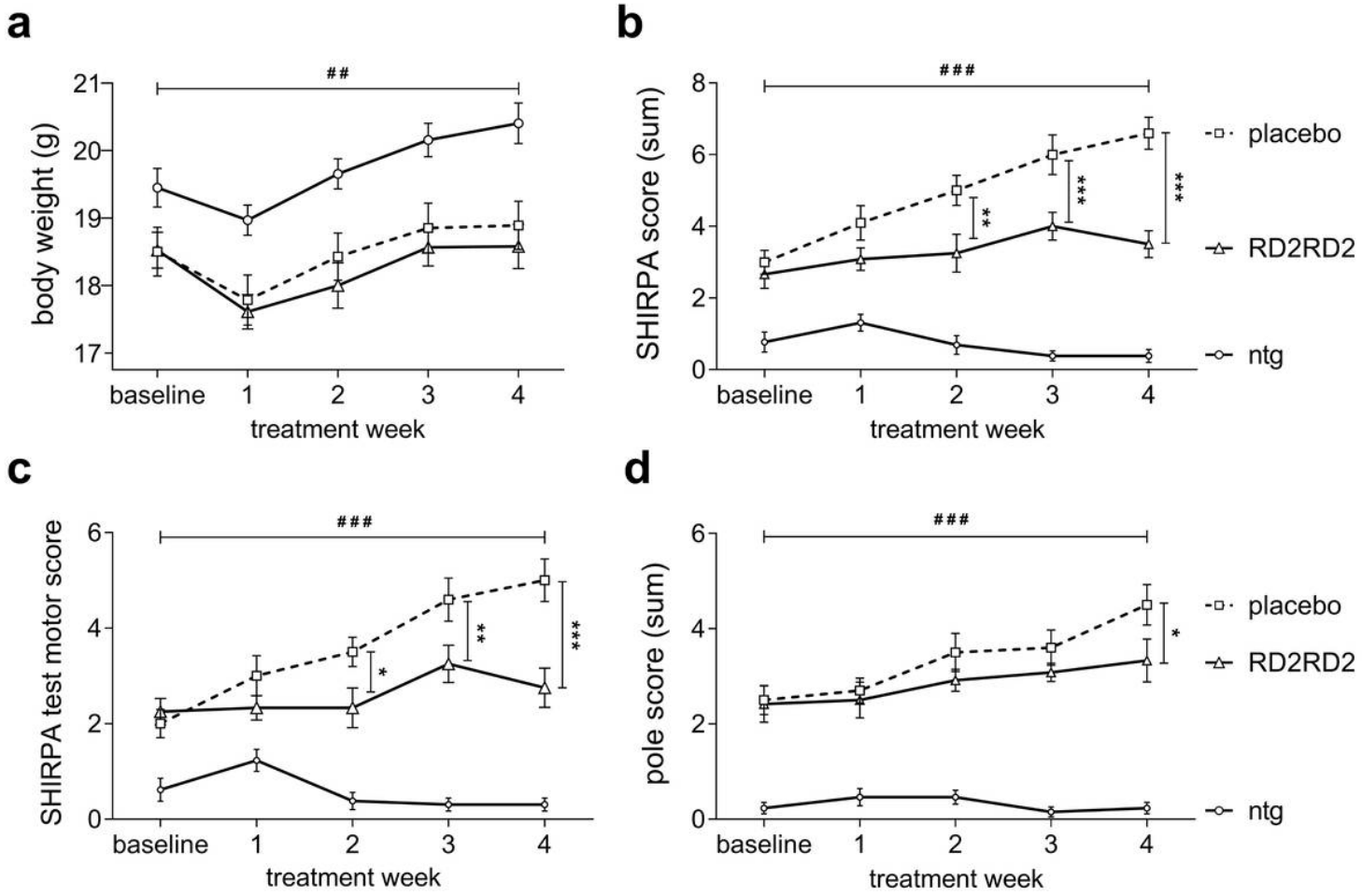

Figure 3

RD2RD2 treatment stopped progression of motor phenotype in SOD1*G93A mice. Changes in absolute body weight (g) over time during treatment revealed significant differences between transgenic and non-transgenic mice (a). Analysis of the SHIRPA test battery to evaluate the phenotypic development of RD2RD2- and placebo-treated SOD1*G93A mice resulted in halt of phenotype progression upon treatment (b). Subdivision of the SHIRPA parameters into a motor score revealed significant inhibition of motor symptom progression in RD2RD2- vs placebo-treated SOD1*G93A (c).Pole test analysis (d) resulted in significant conservation of motor skills in RD2RD2-treated mice, whereas the motor deficits progresses further in placebo-treated mice. All non-transgenic mice exhibited normal motor function throughout the experimental period.Data is presented as mean ± SEM. Statistical calculations were conducted by two-way RM ANOVA with Fisher's LSD post hoc analysis, ntg n = 13, RD2RD2 n = 12 and placebo n = 10 for each test. Lozenges (#) and asterisks (*) indicate a significance between treatment groups (ntg vs RD2RD2 or ntg vs placebo: ## $p < 0.01$, ### $p < 0.001$ and RD2RD2 vs placebo: * $p = 0.05$, ** $p < 0.01$, *** $p < 0.001$)

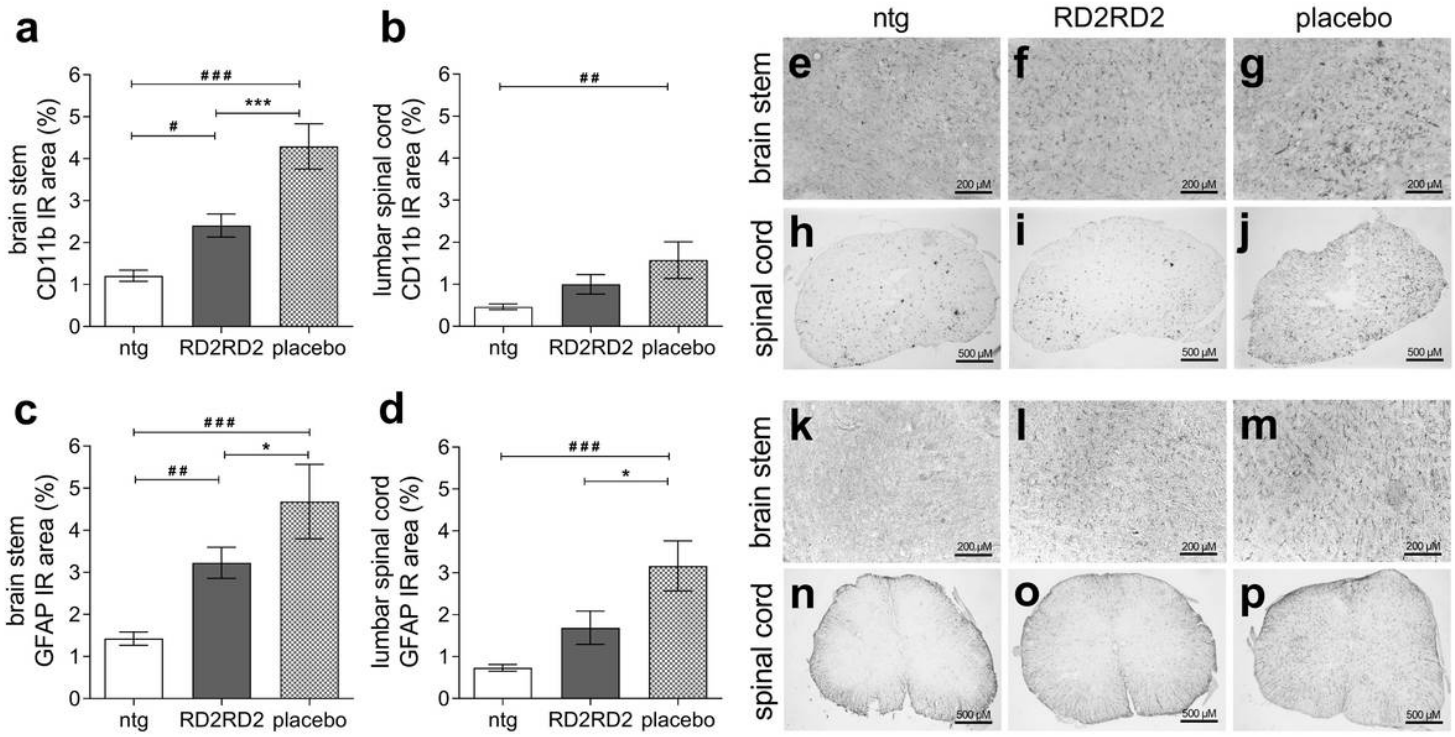

Figure 4

Immunohistochemical investigations revealed reduction of neuroinflammation in RD2RD2-treated SOD1*G93A mice. Analysis of activated microglia and astrocytes in brain stem and lumbar spinal cord showed significant reduction of neuroinflammation (staining with CD11b and GFAP antibodies with subsequent quantification of glia cells). Presentation of the analysed cells, brain and lumbar spinal cord are given on the right (microglia: a, e-g = brain stem and b, h-j = lumbar spinal cord; astrocytes: c, k-m = brain stem and d, n-p = lumbar spinal cord). Data is presented as mean ± SEM. Statistical calculations were conducted by one-way ANOVA with Fisher's LSD post hoc analysis. Lozenges (#) and asterisks (*) indicate a significance between treatment groups (ntg vs RD2RD2 or ntg vs placebo: # $p = 0.05$, ## $p = 0.01$, ### $p < 0.001$ and RD2RD2 vs placebo: * $p = 0.05$, *** $p < 0.001$). IR: immunoreactivity